An Assessment of Traditional and Ensemble Evaporation Models with Implications for Floating Photovoltaic Systems in Northern Cyprus

Youssef Kassem
Department of Mechanical Engineering, Engineering Faculty, Near East University, Nicosia (via Mersin 10, Turkiye), Cyprus | Energy, Environment, and Water Research Center, Near East University, Nicosia (via Mersin 10, Turkiye), Cyprus
yousseuf.kassem@neu.edu.tr (corresponding author)

Huseyin Gokcekus
Department of Civil Engineering, Civil and Environmental Engineering Faculty, Near East University, Nicosia (via Mersin 10, Turkiye), Cyprus | Energy, Environment, and Water Research Center, Near East University, Nicosia (via Mersin 10, Turkiye), Cyprus
huseyin.gokcekus@neu.edu.tr

Abdalla Hamada Abdelnaby Abdelnaby
Department of Civil Engineering, Civil and Environmental Engineering Faculty, Near East University, Nicosia (via Mersin 10, Turkiye), Cyprus
abdalla.hamada@neu.edu.tr

Hasan Yesilyuz
Department of Civil Engineering, Civil and Environmental Engineering Faculty, Near East University, Nicosia (via Mersin 10, Turkiye), Cyprus
20226873@std.neu.edu.tr

Received: 3 January 2026 | Revised: 28 January 2026 | Accepted: 11 February 2026

 DOI: https://doi.org/10.48084/etasr.17322

ABSTRACT

Accurate estimation of evaporation from open water bodies is crucial for sustainable water and energy management, given pronounced seasonal variability and water scarcity. Therefore, the evaporation rate and the performance of seven traditional evaporation estimation models and three ensemble models are assessed at different locations in Northern Cyprus. The results show that the monthly observed evaporation values range from 52.7 to 250 mm. Moreover, it is found that while all methods follow the seasonal pattern of evaporation, there are large differences among them in magnitude. The Penman series models tend to overestimate evaporation, particularly in summer, whereas simpler temperature- and radiation-based methods underestimate peak values. Bayesian Model Averaging (BMA) achieves the best performance, yielding R^2 values of up to 0.997 and reducing RMSE by 30%-45% across ensemble models. Furthermore, the current study aims to assess the techno-economic and environmental viability of small-scale Floating Photovoltaic (FPV) systems on the lakes at Near East University. The results show that higher surface coverage and East-West (E-W) oriented bifacial panel configurations maximize energy generation and improve economic performance while significantly reducing CO_2 emissions. Consequently, a promising avenue for FPV systems toward integrated water-energy sustainability solutions is highlighted.

Keywords-evaporation; ensemble approaches; floating PV system; water-energy sustainability solution

I. INTRODUCTION

A. Background

The process by which water molecules on the surface of a body of water change from liquid to a gaseous state is known as evaporation. It is a component of the hydrological cycle, with important consequences for water resource management [1], climate change research [2, 3], and ecosystem function [4]. The sustainable social and economic advancement of every nation depends on reservoir water supplies. Resources from reservoirs are essential to the long-term social and economic advancement of every nation. Due to the vast open-ocean area, a significant amount of water evaporates annually [5]. Accurately measuring evaporative water loss in reservoirs is, therefore, crucial for managing and using water resources. It can offer basic information and a foundation for protecting water resources [6].

The dynamics of reservoir evaporative water loss depend on both the water surface area and the evaporation rate. However, most current research has focused on variations in the evaporation rate rather than on overall evaporation loss [7]. Reservoir evaporation loss may not be accurately represented by evaporation rates alone, particularly in those reservoirs where floodwater use typically causes significant changes in water surface area. Most studies estimating evaporation losses from reservoirs focus on either large scales (such as the globe or a nation) or point scales (such as an experimental site) [8]. Large-scale studies provide an understanding of terrestrial water surface evaporation at global and national levels. However, the spatiotemporal resolution of such estimates is relatively low, and thus, rapid changes in water surface area and their associated impacts on reservoir evaporation are overlooked. The water surface of a reservoir can change within a few days, which may have considerable impacts on evaporation estimates [9]. Experimental site-scale research yields more precise data; however, data collection is difficult, and such data can only provide limited information on whole-reservoir-scale evaporation [10]. Therefore, to obtain more detailed and continuous evaporation information from the reservoir, high-resolution spatiotemporal data on reservoir surface area and evaporation rate are required [11]. Various methods have been successfully applied to estimate water-surface evaporation rates, including the Pan evaporation method [12], the Eddy Covariance (EC) method [13], the Bowen Ratio Energy Budget (BREB) method [14], the mass balance approach [15], and the Penman equation [16].

One recent innovation in solar power production is the installation of Floating Photovoltaic (FPV) systems on water bodies [17]. The FPV system involves installing solar PV modules on a buoyant surface that floats on water storage structures, including ponds, lakes, reservoirs, and wastewater basins [18]. Installing FPV systems in open reservoirs will not only generate electricity but also lower evaporation by shielding the water's surface from direct sunlight [17,18]. The techno-economic viability of FPV systems at different water bodies has been assessed. Authors in [19] evaluated the economic performance of FPV on Bangladeshi university campuses to offer clean energy and address economic concerns. Authors in [20] investigated the techno-economic feasibility of an FPV plant at the Neel-Nirjan Dam in India.

B. Research Gap and Aim of the Study

In arid and semi-arid areas, reservoirs lose a significant amount of water. These water losses must be accounted for in water resource management, as they significantly affect the regional water balance. Evaporation and transpiration processes in Northern Cyprus have received considerable attention in the literature due to the region's severe water loss and high water demand. Authors in [21] found that the annual evaporation rate was 2220 mm based on Class A Pan readings. Authors in [22] emphasized the importance of accurate evaporation measurement and its application to sustainable groundwater and water resources in ecologically sensitive systems. According to [23], a significant upward trend in potential evapotranspiration was also shown, particularly during dry periods, in regions where water resources are deteriorating, and evaporation is pronounced. Authors in [24] assessed the potential for FPV for evaporation and renewable energy production in Northern Cyprus using a satellite dataset. They found that annual Water Savings (WS) at 100% coverage can amount to 6.21×105 m^3 compared to 0 m^3 in the absence of PV panels. Thus, it is concluded that the comparison of different methods of evaporation estimation and the use of ensemble models to assess their effectiveness against measured evaporation across different regions of Northern Cyprus has not been addressed in the literature. Therefore, the present study aims to evaluate the performance of eight evaporation techniques (Priestley–Taylor, Penman Monteith, Makkink, de Bruin–Keijman, Mass transfer, Blaney-Criddle, de Bruin, and Hamon) utilized to estimate the monthly evaporation from four regions (Güzelyurt, Girne, Gazimağusa, and Lefkoşa) distributed in Northern Cyprus. Additionally, three multi-model ensemble approaches (Median Ensemble, Weighted Ensemble, and Bayesian Model Averaging) are utilized to estimate evaporation and minimize uncertainties associated with individual models (evaporation techniques). Hence, this paper reports a preliminary analysis of the potential to use the best technique, comparing it with available measured data for the selected regions for the first time. Moreover, in alignment with Sustainable Development Goal 7, this study provides a systematic method for assessing the feasibility and effectiveness of small-scale FPV in a water reservoir. To achieve this goal, this study focuses on a specific case involving the reduction of CO_2 emissions and the generation of greener energy on a university campus. Three different floating PV system scenarios are considered in this study. To capture sunlight from both the front and rear sides of the panels, bifacial solar panels are used in both vertical and tilted configurations.

II. MATERIALS AND METHODS

A. Study Area

Cyprus, the third-largest island in the Mediterranean (9,251 km^2), is situated in its eastern basin and has a typical Mediterranean climate with distinct seasonal fluctuations. The hot, dry summers, which last from mid-May to mid-September, are dominated by stable high-pressure systems extending from

Central Asia. As a result, the temperature rises, and the sky is nearly clear. The winter months, from early November to mid-March, which are influenced by a sequence of Mediterranean depressions traveling eastward, receive most of the annual rainfall. Table I shows the geographic information of the selected regions.

TABLE I. SUMMARIZATION OF REGIONS ADOPTED IN THE CURRENT STUDY

Region	Latitude [°N]	Longitude [°E]
Güzelyurt	35.2	32.9
Girne	35.3	33.4
Gazimağusa	35.3	33.8
Lefkoşa	35.2	33.4

B. Climate Parameter

Monthly meteorological information for the selected region (Lefkoşa, Gazimağusa, Girne, and Güzelyurt) was collected from 1982 to 2023 using the NASA POWER dataset and is illustrated in Figure 1. The meteorological data were obtained from NASA [24]. The actual evaporation data from the Meteorological Department station in Lefkoşa were then compared with these estimates.

C. Evaporation Estimation Approaches

A key element of the hydrological cycle, water resource management, and future planning is evaporation (E). The successful operation of the dam system depends on the precise estimation of reservoir evaporation [25]. To estimate water-surface evaporation rates, this study employs various methods.

D. Multi-Method Ensemble for Estimating Evaporation

A multi-method ensemble combines the results of multiple evaporation estimation models into a single, more reliable and accurate prediction than any single technique. These approaches are frequently employed in hydrological, evaporation, and climate-related studies since individual models may have biases, structural limitations, or site-specific deficiencies.

1) Median Ensemble (ME)

ME is one of the simplest and most dependable methods. The ME output is generated by using [26]:

$$E_{ME} = Median\left(E_{1,i}, E_{2,i}, E_{3,i} \ldots E_{N,i}\right) \quad (1)$$

where N is the number of models used for estimating evaporation (E).

2) Weighted Ensemble (WE)

One of the basic WE methods for combining model simulations assigns each model a numerical weight that reflects its relative reliability or skill [27]. Weighted ensembles give greater influence to high-performing models, e.g., those with lower RMSE or higher NSE, to improve prediction robustness while reducing bias [27]. The WE output is generated by using:

$$E_{ME} = \sum_{i=1}^{N} w_i E_i \quad (2)$$

$$w_i = \frac{NSE_i}{\sum_{i=1}^{N} NSE_i} \quad (3)$$

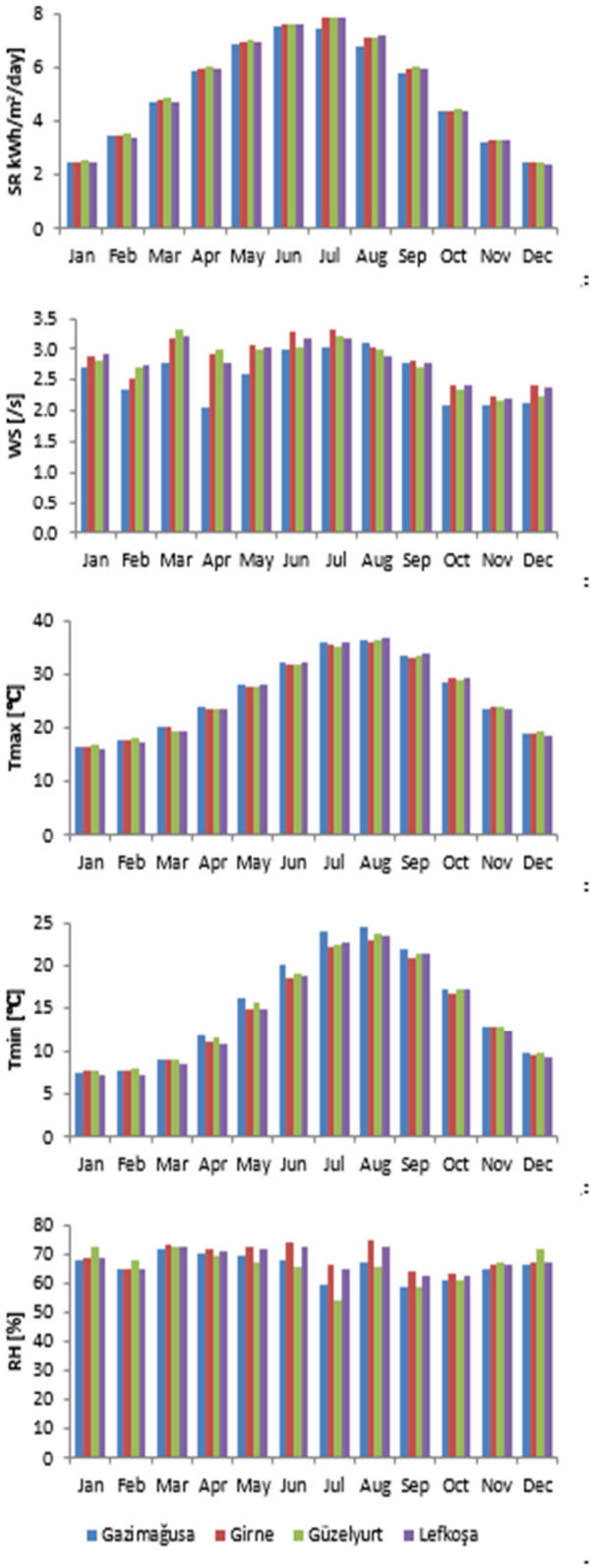

Fig. 1. Monthly variation of climate data.

TABLE II. METHODS USED FOR ESTIMATING EVAPORATION

Method	Equation
Priestley–Taylor	$E = \alpha \cdot \frac{\Delta}{\Delta+\gamma}\left(\frac{R_n - \Delta Q}{\lambda \rho_w}\right) \cdot D$
Penman Monteith	$E = \frac{0.047 \cdot \Delta \cdot R_n + \gamma \cdot \frac{900}{T+273} \cdot U_2 (e_s - e_a)}{\Delta + \gamma \cdot (1 + 0.34 \cdot U_2)}$
Makkink	$E = 0.61 \cdot \frac{\Delta}{\Delta+\gamma} \cdot \frac{R_n}{\lambda} - 0.012$
de Bruin–Keijman	$E = \frac{\Delta}{0.85 \cdot \Delta + 0.63 \cdot \gamma}\left(\frac{R_n - \Delta Q}{\lambda \rho_w}\right) \cdot D$
Mass transfer	$E = 10 \cdot [N U_2 (e_s - e_a)]$
Blaney-Criddle	$E = 25.4(0.0173 T_a - 0.314) T_a \frac{n}{D_{TA}}$
de Bruin	$E = 102.5\left(\frac{\alpha}{\alpha-1}\right)\left(\frac{\gamma}{\Delta+\gamma}\right)\frac{(2.9 + 2.1 U_2)(e_s - e_a)}{\lambda \rho_w}$
Hamon	$E = \frac{35.8 \cdot K \cdot N \cdot e_s}{T + 273.3}$

α: Priestley–Taylor empirically derived constant, dimensionless ($\alpha = 1.26$)
ρ_w: density of water (1000 kg m^{-3})
R_n: the net radiation [W/m^2]
ΔQ: the heat storage change in the water body [W/m^2]
γ: Psychrometric "constant" (depends on temperature and atmospheric pressure) [Pa ℃$^{-1}$]; $\gamma = 0.665 \times 10^{-3} \cdot P$
P: Atmospheric pressure [kPa]
e_s: saturated vapor pressure at temperature of the air [kPa]; $e_s = \frac{1}{2} \cdot \left[0.6108 \cdot exp\left(\frac{17.27 T_{max}}{T_{max}+237.3}\right) + 0.6108 \cdot exp\left(\frac{17.27 T_{min}}{T_{min}+237.3}\right)\right]$
e_a: vapor pressure at temperature and Relative Humidity (RH) of the air [kPa]; $e_a = \frac{RH}{100} \cdot e_s$
Δ: the slope of saturated vapor pressure–air temperature curve [kPa/℃)
λ: the latent heat of vaporization (2.45×10^6 J/kg)
RH: Relative humidity [%]
T_a: Mean air temperature in ℃
D_{TA}: Total annual hours of daylight
n: Actual duration of sunshine in h

3) Bayesian Model Averaging (BMA)

BMA is a probabilistic ensemble method that combines multiple model outputs, weighted by posterior probabilities, which reflect the likelihood that each model is correct given the observed data [28]. Unlike simple or weighted averages, BMA explicitly incorporates model uncertainty by treating the ensemble prediction as a mixture of probability distributions, each model contributing according to its calibrated likelihood. BMA has gained wide acceptance in hydrology and environmental forecasting because it produces probabilistic predictions, quantifies uncertainty, and outperforms deterministic ensembles when inputs are uncertain [28]:

$$E_{BMA} = \sum_{i=1}^{N} \frac{exp(l_i)}{\sum_{i=1}^{N} exp(l_i)} (a_i + b_i E_i) \quad (4)$$

where l_i: log-likelihood of model i.

The line of best fit between measured ($E_{measured}$) and estimated ($E_{estimated}$) is developed as (5) to get the slope (a) and intercept (b):

$$E_{estimated,i} = a_i + b_i E_{measured} \quad (5)$$

E. Basics of Indices Affecting Ranking Method Decision Making

It is significant to use a variety of metrics to measure errors while assessing the prediction ability of the developed models. The mathematical equations of the metrics used are:

$$R^2 = 1 - \frac{\sum_{i=1}^{n} (a_{a,i} - a_{p,i})^2}{\sum_{i=1}^{n} (a_{p,i} - a_{a,ave})^2} \quad (6)$$

$$MSE = \sqrt{\frac{1}{n} \sum_{i=1}^{n} (a_{a,i} - a_{p,i})^2} \quad (7)$$

$$MAE = \frac{1}{n} \sum_{i=1}^{n} |a_{a,i} - a_{p,i}| \quad (8)$$

where n is the number of data, $a_{p,i}$ is the predicted value, $a_{a,i}$ is the actual value, $a_{a,ave}$ is the average actual value, and i is the number of input variables.

F. Case Study

The enhanced PV module efficiency, along with reduced evaporation, represents one of the main advantages of floating PV systems. Additionally, this study assesses the performance of several scenarios for floating PV systems in Northern Cyprus, considering the country's goals for renewable energy exploitation. The lake of Near East University, with an area of 8040 m2, is selected as the case study, as displayed in Figure 2. Near East University is located in the Mediterranean climate zone, which is characterized by hot, dry summers and warm, rainy winters. It is approximately situated at latitude 35.2295° N and longitude 33.3785° E. The monthly variation of meteorological parameters including wind speed, RH, Average temperature (Tave) and Horizontal Solar Irradiance (HIS) is depicted in Figure 3. Water losses due to climate conditions were estimated between 1982 and 2023 using the NASA POWER dataset.

For FPV systems to be effective, long-lasting, and adaptable to various water bodies, the structure and layout are crucial. In this study, three distinct floating PV system scenarios are considered, as portrayed in Figure 4.

In the FPV system, presented in Figure 4, bifacial solar panels are used in both tilted and vertical orientations to capture sunlight on both the front and back sides of the panels. In the case of the tilted bifacial photovoltaic panels, the primary mechanism for sunlight reception is through the direct striking of the sun's rays, and it also makes use of the reflected irradiance from the water body's surface. This design will also positively impact aquatic life. The effect of shading created by the floating system will prevent excessive heating of the water during hot months. This will result in higher dissolved oxygen levels in the water and provide a stable habitat for fish and other aquatic life. Secondly, shading will prevent excessive algal growth in the water. This will be beneficial in maintaining good levels of water quality.

Fig. 2. Lake of Near East University, Northern Cyprus.

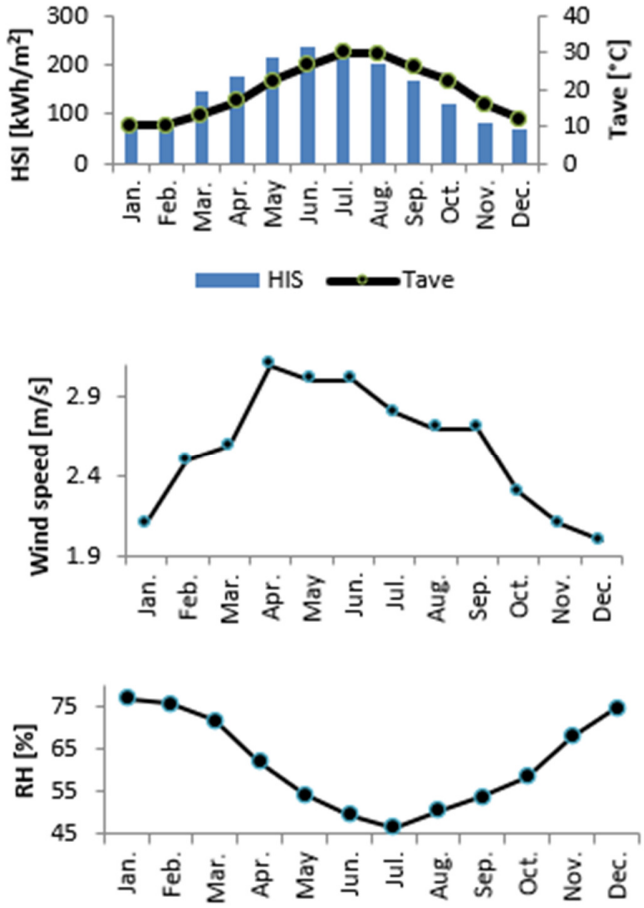

Fig. 3. Monthly variation of weather parameters at the lake of Near East University.

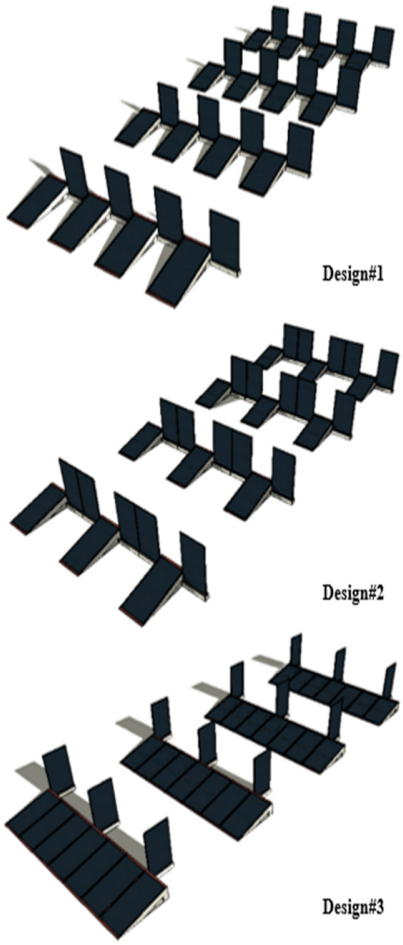

Fig. 4. Lake of Near East University, Northern Cyprus.

The estimated hourly energy output of the floating solar photovoltaic plant will depend on the orientation of the solar arrays. This will include both North-South (N-S) and E-W oriented arrays. For E-W orientation, energy production will be equal in the morning and afternoon, while the N-S orientation will maximize energy production during peak sun irradiation at midday. Based on these two options, the plant's performance can be optimized either for maximum energy production or for uniform hourly energy output. Furthermore, the row spacing is fixed at 3m to avoid shading between the rows, especially in the mornings and afternoons. This row spacing is set to ensure that the tilted and vertical bifacial surfaces of the photovoltaic modules receive adequate levels of direct and reflected irradiance. The row spacing, together with the orientation of the photovoltaic modules, is crucial to minimizing energy losses due to shading. Additionally, it maximizes bifacial gains from reflections off the water surface.

In this work, the proposed system's energy production is estimated using the System Advisor Model (SAM) software. With the software, users can simulate the energy production of mono-facial and bifacial photovoltaic systems, accounting for different system configurations and geographical conditions.

Moreover, WS due to FPVS installation are estimated for four different Covering Ratios (CR) of the lake's surface using [29]:

$$WS = E_{monthly} \times CR \times 0.7 \quad (9)$$

The lake's surface area, as determined using Google Earth, was approximately 8,040 m². The performance of the proposed system was assessed, in this study, using Capacity Factor (CF), Levelized Cost Of Energy ($LCOE$), Simple Payback Period (SPP), and Greenhouse Gas Reduction (GHG_R)[24]:

$$CF = \frac{EP\ [kWh]}{SC\ [kW] \times NH \times ND} \quad (10)$$

$$LCOE = \frac{\sum_{n=0}^{N} \frac{C_n}{(1+r)^n}}{\sum_{n=1}^{N} \frac{Q_n}{(1+r)^n}} \quad (11)$$

$$SPP = \frac{Investment\ cost}{Annual\ Saving} \quad (12)$$

$$GHG_R = (\text{Annual energy generation} \times \text{Emission factor}) - (\text{Annual energy egneration} \times CO_2 \text{ per KWh}) \quad (13)$$

where EP is the energy production from the developed system [kWh], SC is the capacity of the system in kW, NH is the number of hours, ND is the number of days, C_n is the annual project cost in n years, Q_n is the electricity generated by the system in n years, N is the analysis period in years, r is the discount rate, GHG_R is the net CO_2 emission reduction in kg CO_2, and $CO_2\ per\ KWh$ (0.048 kg CO_2/kWh according to Intergovernmental Panel on Climate Change (IPCC), Fifth Assessment Report (AR5).

III. RESULTS

A. Evaporation Results Using Various Methods

Gazimağusa's evaporation data, as illustrated in Figure 5, demonstrate a typical Mediterranean seasonal pattern: low during winter, rising quickly in spring to a peak in midsummer, and dropping gradually in autumn. In winter, the measured values range from 52.7 mm to 250.1 mm in August. All estimating methodologies mimic this seasonal cycle but with considerable variance in amplitude and precision. As shown in Figure 5, the Penman equation consistently yields the highest estimates of evaporation, exceeding the measurements, often more than double in many instances during spring and summer. This implies that Penman may be highly sensitive to the region's high solar radiation and dry summer conditions, overestimating actual surface evaporation when available water is limited. The Priestley-Taylor and Hamon methods also overestimate evaporation compared to observations, although less so than Penman's method. Its high values during summer may reflect its reliance on radiation-dependent processes, which are prevalent under the hot and dry conditions in Gazimagusa. In contrast, the Makkink and Blaney-Criddle methods tend to underestimate evaporation during winter and spring. These simpler models, constrained by temperature or radiation, appear to capture the seasonal trend but not its magnitude, perhaps due to insufficient representation of aerodynamic or humidity effects. Also, the mass transfer methods, de Bruin and de Bruin-Kijman, yield average results and are closer to the measured values in some months. However, their performance was uneven, with lower-than-expected ratings in some months and slightly higher ratings in others.

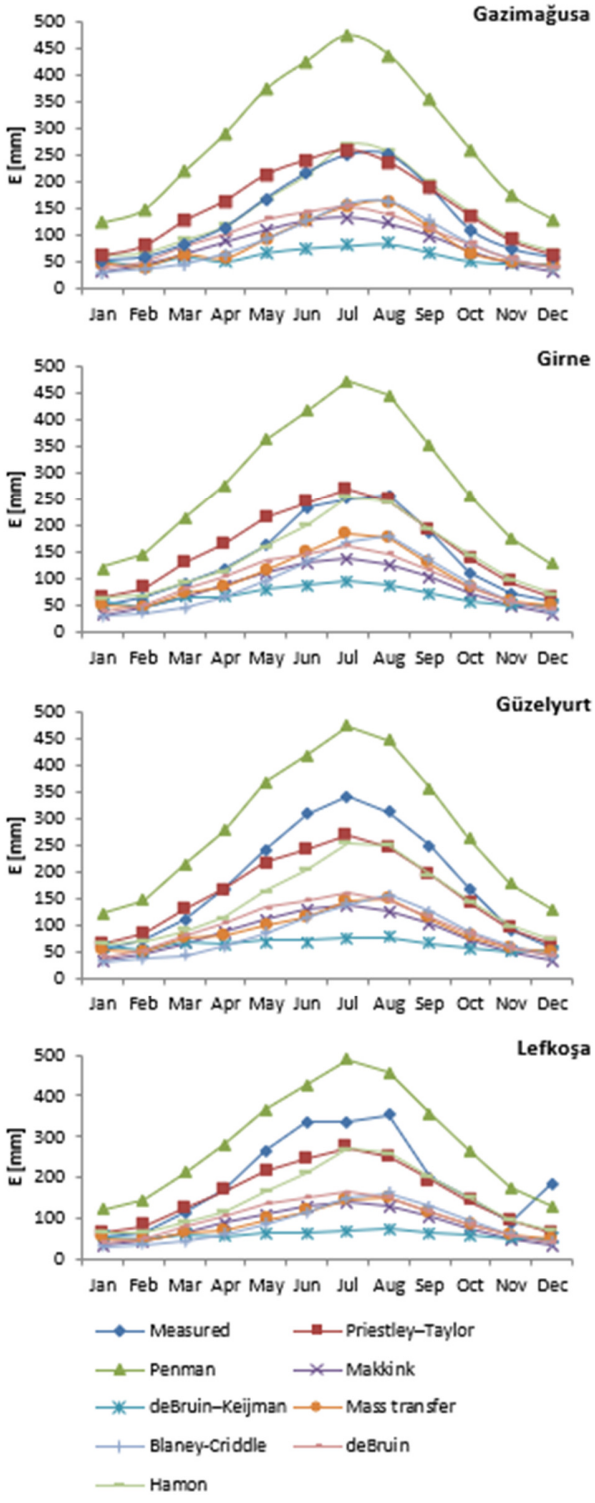

Fig. 5. Monthly variation of measured and estimated values of evaporation for all locations.

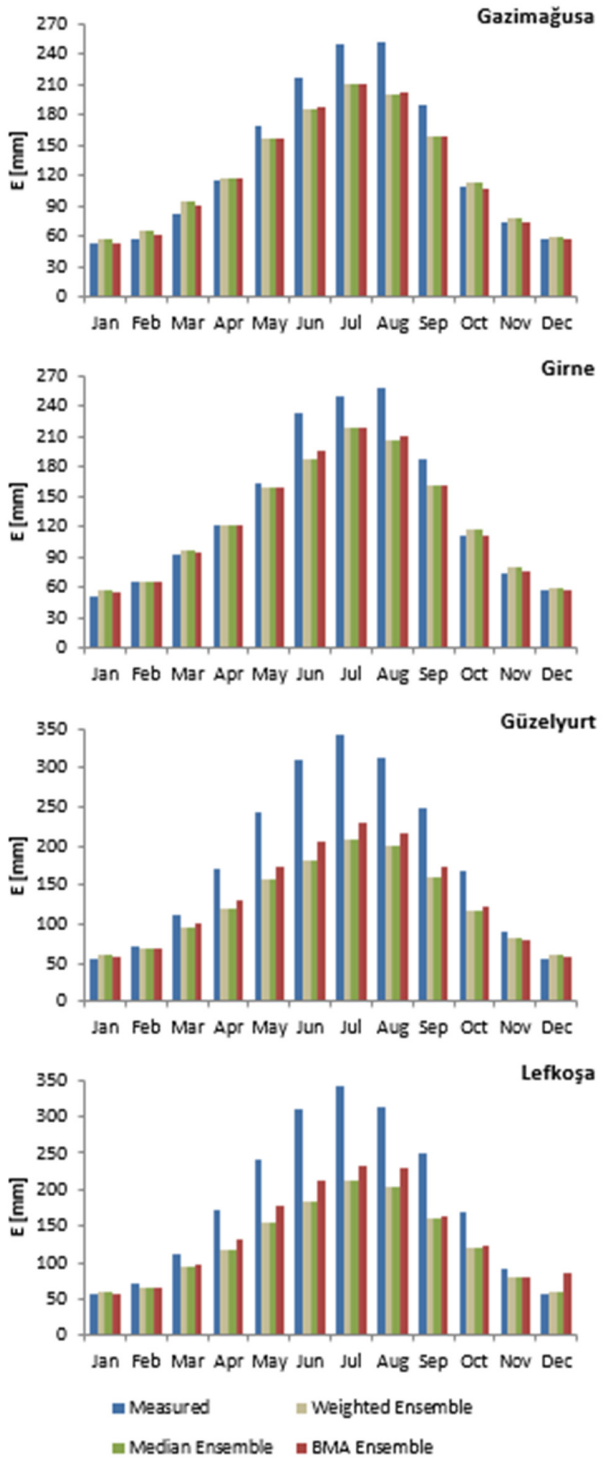

Fig. 6. Monthly variation of measured and estimated values of evaporation using ensemble methods.

B. Evaporation Results Using Ensemble Methods

Figure 6 compares the measured evaporation with the results from three ensemble estimation methods (Weighted, Median, and BMA) for the regions of Gazimağusa, Girne, Güzelyurt, and Lefkoşa. It is found that evaporation exhibits strong seasonal variation, with a minimum during winter (January-February) and a maximum during summer (June-August) in selected regions. The maximum evaporation measured has ranged from 240 to 260 mm in the coastal areas of Gazimağusa and Girne. In contrast, peak values of 300 to 340 mm are observed in the inland areas of Güzelyurt and Lefkoşa. Moreover, the ensemble estimates closely resemble the observed data pattern, indicating that these estimates can effectively capture seasonal variations. Within these ensemble estimates, the weighted and median ensembles slightly underestimate the observations, especially during peak evaporation in the summer. However, the BMA ensemble performs relatively better at estimating the observed data. Differences between data observations and ensemble estimates are relatively small during the winter season but become larger during the summer evaporation periods, when evaporation demand is high. These graphs indicate that ensembles, especially BMA, are a reliable method for estimating evaporation monthly.

C. Best Method for Estimating Evaporation

In this study, the performance statistics for Gazimağusa, Girne, Güzelyurt, and Lefkoşa provide a comprehensive assessment of each method for evaporation estimation and of the ensemble methods, using multiple criteria, including R^2, RMSE, MAE, and RRMSE, as displayed in Figure 7. Hamon is a strong performer relative to the individual models, with the lowest RMSE and MAE values for Gazimağusa and Girne. Also, the Penman model, which has a very high R^2 (>0.96), has an extremely high RMSE. This is similar to these locations for deBruin-Keijman. I found that BMA performs excellently for Gazimağusa and Girne, with large R-squared values (≈0.987) and small RMSE values, indicating superior reliability compared to the individual techniques. For Güzelyurt, the model becomes less accurate, representing the more intricate climate of the interior. The best model is Hamon (R^2=0.954, RMSE=54.679 mm, and MAE=43.480 mm), while the BMA model performs the best (R^2=0.997, RMSE=62.259 mm, and MAE=47.314 mm), significantly improving upon the other techniques. In the case of Lefkoça, the best single model is Hamon (NSE = 0.564); however, the best-performing BMA model achieves the highest R^2, the lowest RMSE, and the lowest MAE among the ensemble methods. In general, the results indicate that although individual methods such as Hamon perform well in particular areas, the best-performing method is, without a doubt, the ensemble method using BMA, as it combines various model-estimation techniques, helping reduce bias and uncertainty.

D. Water Losses and Savings

Table III lists the monthly variation in water loss due to evaporation and the WS that are realized under various FPV surface coverage scenarios (0%, 45%, 60%, 75%, and 100%). Under the baseline case without FPV surface coverage (0%), the annual water loss due to evaporation is 13,325.54 m³, with the highest water loss occurring during the summer season in July and August at 1831.58 m³ and 1718.32 m³, respectively, due to high evaporation demand during hot and dry weather conditions. As FPV surface coverage increases from 45% to

100%, the annual water loss due to evaporation decreases significantly across all months. For 45% FPV surface coverage, the annual water loss decreases to 9127.99 m³, resulting in an annual WS of 4197.54 m³. Also, the annual WS are 5596.73 m³ and 6995.91 m³, respectively, for 60% and 75% FPV surface coverage scenarios. For 100% FPV surface coverage, the annual water loss due to evaporation is significantly reduced to 3997.66 m³, resulting in an annual WS of 9327.88 m³ or 70% compared to the uncovered case.

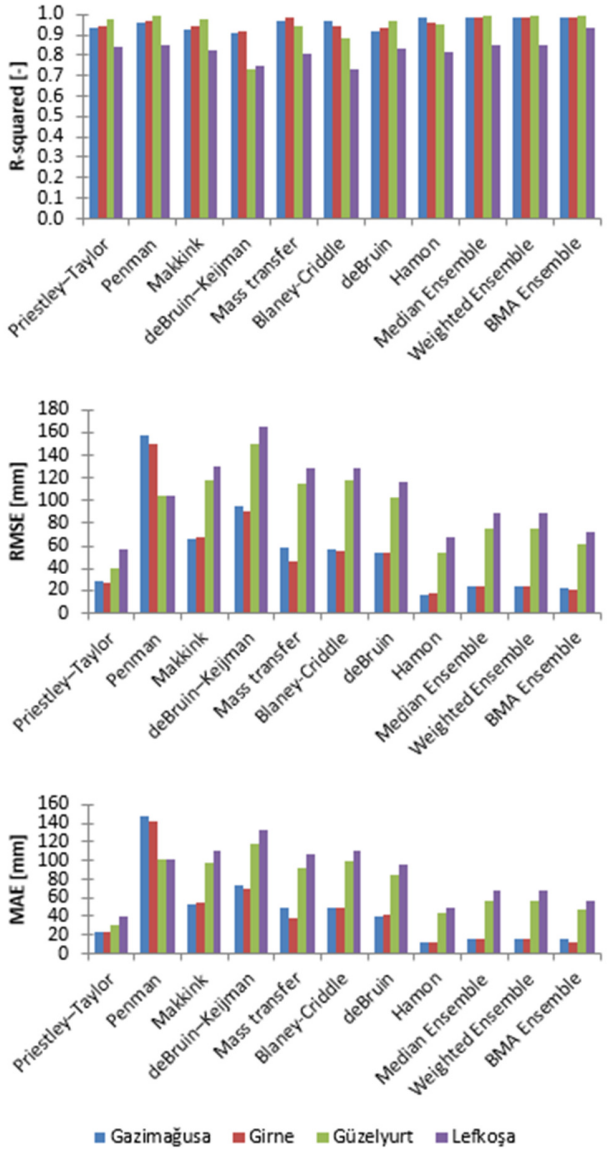

Fig. 7. Monthly variation of climate data. Values of various metrics for measuring the performance of the models.

E. Performance of the Proposed System

The technical performance of the proposed grid-connected photovoltaic system has been evaluated across a variety of scenarios for covering the lake's surface at a chosen site. One of the most effective solar modules, the Bi60-362BSTC (module efficiency = 21.7%), was used in this study, along with a central inverter with a nominal efficiency of 98%. Table IV presents a comparison of the techno-economic and environmental analysis of three types of FPV system designs (Design #1, Design #2, and Design #3), with varying surface coverage ratios (45%, 60%, and 75%) and array pointing (N-S and E-W).

TABLE III. MONTHLY WATER LOSSES AND SAVINGS

Month	**Covering percentage of the Area**				
	0%	45%	60%	75%	100%
Jan	485.63	152.97	203.96	254.96	339.94
Feb	569.90	179.52	239.36	299.20	398.93
Mar	851.59	268.25	357.67	447.09	596.12
Apr	1136.57	358.02	477.36	596.70	795.60
May	1448.56	456.29	608.39	760.49	1013.99
Jun	1675.76	527.86	703.82	879.77	1173.03
Jul	1831.58	576.95	769.26	961.58	1282.11
Aug	1718.32	541.27	721.69	902.12	1202.82
Sep	1394.27	439.19	585.59	731.99	975.99
Oct	1018.00	320.67	427.56	534.45	712.60
Nov	684.89	215.74	287.65	359.57	479.42
Dec	510.48	160.80	214.40	268.00	357.33
WS [m^3]	0.00	4197.54	5596.73	6995.91	9327.88
Water losses [m^3]	13325.54	9127.99	7728.81	6329.63	3997.66

The findings reveal that the effectiveness of the FPV system is significantly affected by the lake surface coverage, as well as the orientation and design of the solar panel array. When the lake surface coverage increases from 45% to 75%, the data demonstrate a significant boost in solar energy production for all three designs, along with an enhanced capacity factor, greater economic viability, and improved qualitative and quantitative measures of environmental impact. Moreover, in all cases, the overall performance of the solar panel system in the E-W orientation has been better than its performance in the N-S orientation, especially at higher levels of coverage, as the solar intensity in the E-W direction varies more evenly in the afternoon as well as in the morning. Among the three designs considered, Design #3 is the best for solar energy production, with an estimated maximum capacity of 594 MWh at 75% lake surface coverage and the highest CF of about 23.45%.

TABLE IV. METHODS USED FOR ESTIMATING EVAPORATION

Parameter	**Covering the lake's surface**	**Design#1**		**Design#2**		**Design#3**	
		N-S	E-W	N-S	E-W	N-S	E-W
EP [MWh]	45%	313	258	289	243	362	356
	60%	417	345	386	324	482	475
	75%	521	431	482	405	603	594
CF [%]	45%	20.58	17.01	19.05	16.01	19.06	23.45
	60%	20.58	17.01	19.05	16.01	19.06	23.45
	75%	20.58	17.01	19.05	16.01	19.06	23.45
SPP [Year]	45%	2.00	2.42	2.16	2.57	1.73	1.75
	60%	1.50	1.81	1.62	1.93	1.30	1.32
	75%	1.20	1.45	1.30	1.54	1.04	1.05
LCOE [cents/kWh]	45%	7.99	9.67	8.64	10.28	6.91	7.02
	60%	6.00	7.25	6.48	7.71	5.18	5.26
	75%	4.80	5.80	5.18	6.17	4.14	4.21
LGHGS [kg CO_2]	45%	3127	2584	2894	2432	3619	3561
	60%	4169	3445	3859	3242	4825	4748
	75%	5211	4307	4823	4053	6031	5936

From an economic viewpoint, increased surface coverage significantly reduces the SPP and LCOE. The payback period drops to about 1 year at 75% coverage for Design #3. At the same time, LCOE drops to around 4.2–4.4 cents/kWh, positioning this configuration as the most economically efficient one among the options studied. On the contrary, Design #2 exhibits somewhat higher LCOE values and longer payback periods, indicating lower economic efficiency. Such trends confirm the importance of optimized geometry and orientation towards better financial viability of floating PV installations.

Regarding environmental performance, the reduction in greenhouse gas emissions over the structure's life span increases proportionally with the amount of energy generated. In this regard, design #3 ensures maximum emission reduction, exceeding 6000 kg of CO_2 at 75% coverage, thus highlighting the potential of such designs in fighting climate change. In fact, designs ensure substantial environmental gains without

IV. DISCUSSION

The outcomes of this research confirm that the estimation of evaporation in Mediterranean, water-limited regions is highly sensitive to the choice of the model. In line with previous findings indicating substantial differences in evaporation estimates for arid regions from different evaporation models, the current results show that while all methods successfully identify the seasonal trend, their amplitudes vary considerably [30-32]. Additionally, the Penman-Monteith model is considered reliable for estimating evaporation. Still, it tends to overestimate actual evaporation under water-limited conditions [33-36]. This overestimation is due to the model's high sensitivity to water requirements under these conditions, as well as to solar radiation [33-36]. In contrast, simpler temperature- and radiation-index methods, such as the Makkink and Blaney-Criddle methods, tend to underestimate maximum evaporation, primarily because they are insensitive to humidity and aerodynamic effects [37-39]. Using ensemble methods is a definite improvement over other methods, thereby supporting the existing literature on the use of multi-model methods to reduce uncertainty in hydrological modeling [40,41]. The BMA method performs better in terms of goodness of fit as well as the error measures, thereby highlighting its capacity to combine the strengths of various models. By expanding the application to include renewable energy, the evaluation of the FPV system confirms that increasing the solar array coverage area leads to higher energy production and greater financial efficiency, consistent with the findings in [24,29]. This study's results show that designing a high-coverage, E-W oriented bifacial system maximizes energy production and reduces the levelized cost of electricity and carbon dioxide emissions.

V. CONCLUSIONS

This study provided an analysis of conventional and ensemble techniques for estimating evaporation, and their implications for implementing Floating Photovoltaic (FPV) systems in a Mediterranean climate. Although individual evaporation models yield satisfactory results for seasonal changes, their outputs vary widely in magnitude, leading to confusion and uncertainty when estimating water resources and FPV performance. The results show that ensemble modeling, particularly Bayesian Model Averaging (BMA), is the most accurate method for estimating evaporation, thereby greatly reducing uncertainty. The implementation of accurate evaporation estimation techniques for FPV systems has shown that maximum surface coverage and East-West (E-W) orientation have the greatest impact on energy production, the levelized cost of electricity, the payback period, and evaporation mitigation for water resources. These findings have proven the dual benefits of FPV systems for water resource management and renewable energy production. Consequently, the results of this research support the implementation of ensemble-based evaporation estimation as the best practice for water-energy planning in Mediterranean and other water-stressed regions.

VI. LIMITATIONS AND FUTURE WORK

This research has limitations that should be considered when analyzing the results. Initially, the analysis of evaporation is based on monthly data, which may not capture short-term changes or extreme climatic conditions that affect water-energy interaction. Secondly, the analysis is conducted under Mediterranean climatic conditions, and the research's applicability to other climates should be further investigated. Finally, while the ensemble approach reduces uncertainty compared to using individual methods, the analysis is limited to conventional evaporation methods, whereas advanced methods, including data-driven and physically based methods, are not considered. Future studies should incorporate higher-resolution meteorological and remote-sensing data to improve the accuracy of evaporation estimates, thereby enabling better planning of water-energy systems. In addition, measurements of long-term evaporation reduction under FPV installations are also proposed. In terms of policy, this approach could be extended to other locations to facilitate informed decision-making on FPV implementation, thereby enabling climate-resilient energy planning and water resource management, as desired by the country's energy transition policy and Sustainable Development Goal 7.

REFERENCES

[1] K. Friedrich *et al.*, "Reservoir Evaporation in the Western United States: Current Science, Challenges, and Future Needs," *Bulletin of the American Meteorological Society*, vol. 99, no. 1, pp. 167–187, Jan. 2018, https://doi.org/10.1175/BAMS-D-15-00224.1.

[2] A. Dai, T. Zhao, and J. Chen, "Climate Change and Drought: a Precipitation and Evaporation Perspective," *Current Climate Change Reports*, vol. 4, no. 3, pp. 301–312, Sept. 2018, https://doi.org/10.1007/s40641-018-0101-6.

[3] Q. Wang, H. Deng, and J. Jian, "Hydrological Processes under Climate Change and Human Activities: Status and Challenges," *Water*, vol. 15, no. 23, p. 4164, Jan. 2023, https://doi.org/10.3390/w15234164.

[4] H. Zhang, S. M. Gorelick, P. V. Zimba, and X. Zhang, "A remote sensing method for estimating regional reservoir area and evaporative loss," *Journal of Hydrology*, vol. 555, pp. 213–227, Dec. 2017, https://doi.org/10.1016/j.jhydrol.2017.10.007.

[5] S. Zhan, C. Song, J. Wang, Y. Sheng, and J. Quan, "A Global Assessment of Terrestrial Evapotranspiration Increase Due to Surface Water Area Change," *Earth's Future*, vol. 7, no. 3, pp. 266–282, Mar. 2019, https://doi.org/10.1029/2018EF001066.

[6] L. Zhou, L. Cheng, S. Qin, Y. Mai, and M. Lu, "Estimation of Urban Evapotranspiration at High Spatiotemporal Resolution and Considering Flux Footprints," *Remote Sensing*, vol. 15, no. 5, Jan. 2023, Art. no. 1327, https://doi.org/10.3390/rs15051327.

[7] G. Zhao, H. Gao, and X. Cai, "Estimating lake temperature profile and evaporation losses by leveraging MODIS LST data," *Remote Sensing of Environment*, vol. 251, Dec. 2020, Art. no. 112104, https://doi.org/10.1016/j.rse.2020.112104.

[8] Y. Wang, O. Merlin, G. Zhu, and K. Zhang, "A Physically Based Method for Soil Evaporation Estimation by Revisiting the Soil Drying Process," *Water Resources Research*, vol. 55, no. 11, pp. 9092–9110, Oct. 2019, https://doi.org/10.1029/2019WR025003.

[9] D. Althoff, L. N. Rodrigues, and D. D. da Silva, "Impacts of climate change on the evaporation and availability of water in small reservoirs in the Brazilian savannah," *Climatic Change*, vol. 159, no. 2, pp. 215–232, Mar. 2020, https://doi.org/10.1007/s10584-020-02656-y.

[10] F. Chen *et al.*, "Modeling of land surface evaporation by four schemes and comparison with FIFE observations," *Journal of Geophysical Research: Atmospheres*, vol. 101, no. D3, pp. 7251–7268, Mar. 1996, https://doi.org/10.1029/95JD02165.

[11] G. Zhao and H. Gao, "Estimating reservoir evaporation losses for the United States: Fusing remote sensing and modeling approaches," *Remote Sensing of Environment*, vol. 226, pp. 109–124, Jun. 2019, https://doi.org/10.1016/j.rse.2019.03.015.

[12] M. Kohler, T.J. Nordenson, W.E. Fox, *Evaporation from Pans and Lakes, 1st ed. Washington, D.C, USA: Department of Commerce, 1955.*

[13] P. D. Blanken *et al.*, "Eddy covariance measurements of evaporation from Great Slave Lake, Northwest Territories, Canada," *Water Resources Research*, vol. 36, no. 4, pp. 1069–1077, Apr. 2000, https://doi.org/10.1029/1999WR900338.

[14] J. Finch and A. Calver, *Methods for the quantification of evaporation from lakes*, 1st ed. Oxfordshire, UK: CEH Wallingford, 2008.

[15] W. Brutsaert, *Evaporation into the Atmosphere*. Dordrecht: Springer Netherlands, 1982.

[16] H. L. Penman, "Natural evaporation from open water, bare soil and grass," *Proceedings of the Royal Society of London. A. Mathematical and Physical Sciences*, vol. 193, no. 1032, pp. 120–145, Apr. 1948, https://doi.org/10.1098/rspa.1948.0037.

[17] J. Dellosa and E. V. Palconit, "Resource Assessment of a Floating Solar Photovoltaic (FSPV) System with Artificial Intelligence Applications in Lake Mainit, Philippines," *Engineering, Technology & Applied Science Research*, vol. 12, no. 2, pp. 8410–8415, Apr. 2022, https://doi.org/10.48084/etasr.4863.

[18] R. Cáceres González *et al.*, "Exploring climate-driven performance of floating photovoltaic systems: Energy production enhancement and evaporation reduction," *Applied Energy*, vol. 386, May 2025, Art. no. 125556, https://doi.org/10.1016/j.apenergy.2025.125556.

[19] A. Jawad, Md. S. Hasan, Md. F. I. Faruqui, and N.-A.- Masood, "Small-scale floating photovoltaic systems in university campus: A pathway to achieving SDG 7 goals in Bangladesh," *Energy Conversion and Management*, vol. 297, Dec. 2023, Art. no. 117722, https://doi.org/10.1016/j.enconman.2023.117722.

[20] A. Goswami, P. Sadhu, U. Goswami, and P. K. Sadhu, "Floating solar power plant for sustainable development: A techno-economic analysis," *Environmental Progress & Sustainable Energy*, vol. 38, no. 6, May 2019, Art. no. e13268, https://doi.org/10.1002/ep.13268.

[21] G. Elkiran and M. Ergil, "The assessment of a water budget of North Cyprus," *Building and Environment*, vol. 41, no. 12, pp. 1671–1677, Dec. 2006, https://doi.org/10.1016/j.buildenv.2005.06.014.

[22] T. A. Endreny, "Estimating recharge rates for qanat-based water supply in northern Cyprus: a case study using remotely sensed and in-situ data," *Urban Water Journal*, vol. 5, no. 2, pp. 161–171, Jun. 2008, https://doi.org/10.1080/15730620701754202.

[23] B. Koyuncu, " Evapotranspiration analysis of North Cyprus," M.S. thesis, Middle East Technical University, Ankara, Turkey, 2019.

[24] Y. Kassem, H. Gökçekuş, and R. Gökçekuş, "Towards Sustainable Energy Solutions: Evaluating the Impact of Floating PV Systems in Reducing Water Evaporation and Enhancing Energy Production in Northern Cyprus," *Energies*, vol. 17, no. 21, Jan. 2024, Art. no. 5300, https://doi.org/10.3390/en17215300.

[25] M. F. Allawi, M. L. Ahmed, I. A. Aidan, R. C. Deo, and A. El-Shafie, "Developing reservoir evaporation predictive model for successful dam management," *Stochastic Environmental Research and Risk Assessment*, vol. 35, no. 2, pp. 499–514, Feb. 2021, https://doi.org/10.1007/s00477-020-01918-6.

[26] L. Shandross *et al.*, "Multi-model ensembles in infectious disease and public health: Methods, interpretation, and implementation in R." medRxiv, May 2025, Art. no. 2024.06.24.24309416, https://doi.org/10.1101/2024.06.24.24309416.

[27] Y. Wang, Y.-J. Shen, L. Wang, Y. Guo, Y. Cheng, and X. Zhang, "Multi-Model Ensemble Enhances the Spatiotemporal Comprehensive Performance of Regional Climate in China," *Remote Sensing*, vol. 17, no. 4, Jan. 2025, Art. no. 582, https://doi.org/10.3390/rs17040582.

[28] A. E. Raftery, T. Gneiting, F. Balabdaoui, and M. Polakowski, "Using Bayesian Model Averaging to Calibrate Forecast Ensembles," *Monthly Weather Review*, vol. 133, no. 5, pp. 1155–1174, May 2005, https://doi.org/10.1175/MWR2906.1.

[29] H. F. Abd-Elhamid, A. Ahmed, M. Zeleňáková, Z. Vranayová, and I. Fathy, "Reservoir Management by Reducing Evaporation Using Floating Photovoltaic System: A Case Study of Lake Nasser, Egypt," *Water*, vol. 13, no. 6, Jan. 2021, Art. no. 769, https://doi.org/10.3390/w13060769.

[30] A. Bozorgi, O. Bozorg-Haddad, S. Sima, and H. A. Loáiciga, "Comparison of methods to calculate evaporation from reservoirs," *International Journal of River Basin Management*, vol. 18, no. 1, pp. 1–12, Jan. 2020, https://doi.org/10.1080/15715124.2018.1546729.

[31] D. L. McJannet, F. J. Cook, and S. Burn, "Comparison of techniques for estimating evaporation from an irrigation water storage," *Water Resources Research*, vol. 49, no. 3, pp. 1415–1428, Feb. 2013, https://doi.org/10.1002/wrcr.20125.

[32] S. Ali, N. C. Ghosh, and R. Singh, "Evaluating best evaporation estimate model for water surface evaporation in semi-arid region, India," *Hydrological Processes*, vol. 22, no. 8, pp. 1093–1106, Aug. 2007, https://doi.org/10.1002/hyp.6664.

[33] T. A. Chauhan, S. A. Ghausi, A. Hildebrandt, and A. Kleidon, "Correcting overestimated potential evaporation from the Penman-Monteith equation during water-limited conditions," Copernicus Meetings, EGU25-10825, Mar. 2025, https://doi.org/10.5194/egusphere-egu25-10825.

[34] Y. Aydın, "Assessing of evapotranspiration models using limited climatic data in Southeast Anatolian Project Region of Turkey," *PeerJ*, vol. 9, Jun. 2021, Art. no. e11571, https://doi.org/10.7717/peerj.11571.

[35] M. Irizarry-Ortiz and E. W. Harmsen, "Sensitivity of the Penman–Monteith Reference Evapotranspiration Equation to Meteorological Variables for Puerto Rico," *Hydrology*, vol. 10, no. 5, May 2023, Art. no. 101, https://doi.org/10.3390/hydrology10050101.

[36] S. Zhou and B. Yu, "Physical basis of the potential evapotranspiration and its estimation over land," *Journal of Hydrology*, vol. 641, Sept. 2024, Art. no. 131825, https://doi.org/10.1016/j.jhydrol.2024.131825.

[37] G. Kountios, I. Chatzis, C. Konstantinidis, M. Tsiouni, A. Kontogeorgos, and G. Papadavid, "Irrigation plan for cotton farm in Palamas, Karditsa prefecture, Thessaly, Greece," in *Ninth International Conference on Remote Sensing and Geoinformation of the Environment (RSCy2023)*, Sept. 2023, vol. 12786, pp. 606–614, https://doi.org/10.1117/12.2682691.

[38] S. J. Acquah *et al.*, "Application and evaluation of Stanghellini model in the determination of crop evapotranspiration in a naturally ventilated greenhouse," *International Journal of Agricultural and Biological Engineering*, vol. 11, no. 6, pp. 95–103, Dec. 2018.

[39] R. López-Urrea, F. Olalla, C. Fabeiro, and A. Moratalla, "An evaluation of two hourly reference evapotranspiration equations for semiarid conditions," *Agricultural Water Management*, vol. 86, pp. 277–282, Dec. 2006, https://doi.org/10.1016/j.agwat.2006.05.017.

[40] J. De Niel, E. Van Uytven, and P. Willems, "Uncertainty Analysis of Climate Change Impact on River Flow Extremes Based on a Large Multi-Model Ensemble," *Water Resources Management*, vol. 33, no. 12,

pp. 4319–4333, Sept. 2019, https://doi.org/10.1007/s11269-019-02370-0.

[41] Y. Wan *et al.*, "Performance dependence of multi-model combination methods on hydrological model calibration strategy and ensemble size," *Journal of Hydrology*, vol. 603, Dec. 2021, Art. no. 127065, https://doi.org/10.1016/j.jhydrol.2021.127065.